



Identifying motor functional neurological disorder using resting-state functional connectivity



Jennifer Wegrzyk^{a,1}, Valeria Kebets^{b,1}, Jonas Richiardi^b, Silvio Galli^a, Dimitri Van de Ville^{c,d}, Selma Aybek^{a,b,e,*}

^a Department of Clinical Neuroscience, Geneva University Hospital, Rue Gabrielle-Perret-Gentil 4, 1211 Geneva, Switzerland

^b Department of Neuroscience, University of Geneva, Campus Biotech, Chemin des Mines 9, 1202 Geneva, Switzerland

^c Institute of Bioengineering, Ecole Polytechnique Fédérale de Lausanne, Campus Biotech, Chemin des Mines 9, 1202 Geneva, Switzerland

^d Department of Radiology and Medical Informatics, University of Geneva, Campus Biotech, Chemin des Mines 9, 1202 Geneva, Switzerland

^e Neurology University Clinic, InselSpital, Department of Clinical Neuroscience, 3010 Bern, Switzerland

ARTICLE INFO

Keywords:

Resting state functional magnetic resonance imaging
Functional connectivity
Functional neurological disorder
Biomarker
Classification

ABSTRACT

Background: Motor functional neurological disorder (mFND) is a clinical diagnosis with reliable features; however, patients are reluctant to accept the diagnosis and physicians themselves bear doubts on potential misdiagnoses. The identification of a positive biomarker could help limiting unnecessary costs of multiple referrals and investigations, thus promoting early diagnosis and allowing early engagement in appropriate therapy.

Objectives: To test whether resting-state (RS) functional magnetic resonance imaging could discriminate patients suffering from mFND from healthy controls.

Methods: We classified 23 mFND patients and 25 age- and gender-matched healthy controls based on whole-brain RS functional connectivity (FC) data, using a support vector machine classifier and the standard Automated Anatomic Labeling (AAL) atlas, as well as two additional atlases for validation.

Results: Accuracy, specificity and sensitivity were over 68% ($p = 0.004$) to discriminate between mFND patients and controls, with consistent findings between the three tested atlases. The most discriminative connections comprised the right caudate, amygdala, prefrontal and sensorimotor regions. Post-hoc seed connectivity analyses showed that these regions were hyperconnected in patients compared to controls.

Conclusions: The good accuracy to discriminate patients from controls suggests that RS FC could be used as a biomarker with high diagnostic value in future clinical practice to identify mFND patients at the individual level.

1. Introduction

Motor functional neurological disorder (mFND) – formerly called “hysteria” – represents a clinical diagnosis for which positive bedside signs exist (Daum et al., 2014), and treating clinicians, mostly neurologists and psychiatrists, can refer to established diagnostic criteria (Diagnostic and Statistical Manual of Mental Disorders (DSM-5)). Even though misdiagnosis rates are low (Stone et al., 2009), neurologists still fear missing an underlying organic pathology (Slater, 1965) and a majority continue to engage in an exclusionary process involving many additional investigations (Espay et al., 2009). A misdiagnosis in the other direction – i.e., diagnosing an organic disease when the actual diagnosis is mFND – can also have serious consequences for the patients as this results in unnecessary treatments such as thrombolysis

(Vroomen et al., 2008). Appropriate therapy is then delayed, which importantly impacts outcome (Gelauff et al., 2014) and societal costs (Carson et al., 2011).

Besides the fear of misdiagnosis, neurologists avoid discussing the diagnosis of functional neurological disorder (FND) with their patients (Kanaan et al., 2009a) because they themselves bear doubts about an alternate explanation for the symptoms of feigning (Kanaan et al., 2009b). Patients in turn feel their doctors do not understand them, which leads to multiple consultations for the same symptoms and change of general practitioner (Crimlisk et al., 2000). The identification of a positive biomarker for mFND could strengthen the physician's clinical diagnosis and reassure the patients, thus limiting unnecessary costs of multiple referrals and investigations, promoting an early diagnosis and allowing early engagement in appropriate therapy.

* Corresponding author at: Universitätsklinik für Neurologie, Department of Clinical Neuroscience, InselSpital, 3010 Bern, Switzerland.

E-mail address: selma.aybek@insel.ch (S. Aybek).

¹ These authors contributed equally to the manuscript.

A new and promising tool in the search of biomarkers for neuropsychiatric disorders is resting-state (RS) functional magnetic resonance imaging (fMRI) (Woodward and Cascio, 2015) which allows the study of blood oxygen level dependent (BOLD) signal fluctuations generated under resting conditions. The temporal correlation between the time courses of different brain regions is computed to obtain measures of functional connectivity (FC). Compared to active tasks, the advantage of RS fMRI is that behavioral differences between patients and controls have lower impact on the interpretation of the results.

Literature in functional neuroimaging of mFND has been dominated by task-based studies, all aiming at uncovering the neural correlates of the disorder. Two RS studies in mFND patients (Maurer et al., 2016; Baek et al., 2017) have investigated neural correlates of the disorder but no studies to date have used a multivariate classification approach to investigate RS FC as a potential positive biomarker. The aim of our study was therefore to use whole-brain RS FC in a predictive setting to discriminate mFND patients from healthy controls.

2. Methods and materials

2.1. Participants

53 subjects (26 mFND patients and 27 controls matched for age and gender) participated in the study (Table 1). Three patients (1 patient with movement disorders and 2 patients with weakness) and 2 healthy controls were excluded from analysis due to excessive movement in the scanner, resulting in a total sample of 48 subjects. Patients were recruited from the outpatient clinic of a tertiary university hospital (University Hospitals Geneva, Department of Clinical Neurosciences). Two board-certified neurologists (SG or SA) confirmed the diagnosis of FND according to DSM-5 criteria and using motor positive signs (e.g., Hoover sign or tremor variability, distractibility and entrainment test). Healthy control subjects (with a similar sociodemographic background and individually matched to the patients by age and sex) were recruited via advertisement. For both groups, the main exclusion criteria were current neurological disorders, substance dependence and contraindications for MRI scanning. The study was approved by the ethics committee of the University Hospitals of Geneva (CER 14-088). All participants gave written informed consent in accordance with the Declaration of Helsinki.

2.2. Data acquisition

2.2.1. Clinical evaluation

Participants completed the State Anxiety Inventory (STAI-S) (CDG et al., 1983) and the Beck Depression Inventory (BDI) (Beck et al., 1996) on the day of MRI session. Clinical severity of the motor

Table 1
Demographic values and clinical scores.

	mFND patients (n = 23)	Healthy controls (n = 25)	P-value
Age, mean (SD), years	42.4 (13.9)	42.4 (13.0)	0.985
Gender (females/males)	21/2	22/3	0.708
Type of symptom	11 weakness 12 tremor/jerks/ dystonia	NA	
Disease severity (median CGI)	2	NA	
Disease duration, mean (SD), months	4.8 (6.3)	NA	
BDI score, mean (SD)	7.5 (5.2)	1.9 (6.1)	< 0.001 ^a
STAI-S score, mean (SD)	34.8 (9.4)	34(8.1)	0.940

STAI-S: Anxiety State value, BDI: Beck Depression Index, CGI: Clinical Global Impression. SD = standard deviation; NA = not applicable.

^a Significantly different between groups.

symptom was evaluated by the neurologists with a 0–5 Clinical Global Impression Score (CGI) (0 = no symptom to 5 = very disabling symptom).

2.2.2. MRI acquisition parameters

MRI was performed using a 3.0 Tesla unit (Siemens, Magnetom TrioTim). Functional imaging data and one structural image were acquired in one session. fMRI data were acquired using a whole-brain single shot multi-slice BOLD echo-planar-imaging (EPI) sequence with the following parameters: TR: 2 s; TE: 20 ms; flip angle 80°; PAT factor = 2; FOV: 240 mm; matrix size: 64 × 64 × 40; 2.5 mm slice thickness; interslice gap 1.1125 mm; voxel size 3.00 × 3.00 × 2.50 mm; TA: 5:08 min, 150 functional images.

During the RS fMRI session, the subjects were instructed to lie still, to think of nothing in particular and to watch a cross symbol projected on a black screen. The scan protocol for structural MRI consisted of a T1-weighted MPRAGE sequence with the following parameters: TR: 1.9 s; TE: 2.27 ms; flip angle = 9°; PAT factor = 2, voxel size 1.0 × 1.0 × 1.0 mm; acquisition time: 5:04.

2.3. Data analyses

Demographic and clinical data were compared between the two groups with two-sample *t*-tests or Mann-Whitney *U* tests (depending on the distribution normality), and the chi2 test when appropriate.

2.3.1. Preprocessing of imaging data

For preprocessing, we relied on a previously used pipeline (Richiardi et al., 2012) using SPM12 tools (<http://www.fil.ion.ucl.ac.uk/spm/software/spm12/>). Functional images were first realigned, then the mean functional image was co-registered with the structural image. The latter was segmented into grey matter, white matter, and cerebrospinal fluid. A customized version of the IBASPM toolbox (Aleman-Gomez et al., 2006) was used to build an individual structural brain atlas, based on the AAL atlas (Tzourio-Mazoyer et al., 2002). In order to check the consistency of the results, two other atlases, the Hammers probabilistic structural atlas (Hammers et al., 2003), and the Shirer functional atlas (Shirer et al., 2012), were additionally chosen for comparison. The atlas was then mapped back onto the native resolution of the functional data, and region-averaged time series were extracted. The first 10 time points were discarded to ensure magnetization equilibrium. Motion parameters, as well as the average signal of a mask of white matter and cerebrospinal fluid, were regressed out. Time series were Winsorized to the 95th percentile to increase robustness to outliers (e.g., spikes). Time courses were then filtered into frequency subbands using a wavelet transform (cubic orthogonal B-spline wavelets). Five frequency subbands were extracted, respectively with main bandpass characteristics at 0.5–1 Hz, 0.25–0.5 Hz, 0.125–0.25 Hz, 0.0625–0.125 Hz, and 0.0312–0.0625 Hz. We investigated alterations of FC in the latter subband (0.0312–0.0625 Hz), as this subband represents typical low-frequency RS fluctuations. Motion-related artefacts were accounted for as described in Supplemental File Appendix 1.

2.3.2. RS FC modelling and classification

We computed pairwise Pearson correlation coefficients between all atlas regions in order to obtain a correlation matrix (number of regions × number of regions) for each subject (see Supplemental File, Appendix 2). Next, we converted the correlation coefficients to z-scores using Fisher-Z transformation, and used them as features for the classifier by reshaping the upper-triangular part of the matrix (excluding the diagonal) as a vector.

We used a linear Support Vector Machine (SVM) classifier with L2 regularization to learn a discriminant function that would optimally separate the two groups. The SVM is a supervised learning method that performs binary classification, by building the largest-margin hyperplane allowing for an optimal separation of the training examples. We

used the SVM implementation of the LIBSVM package (<http://www.csie.ntu.edu.tw/~cjlin/libsvm>) while setting the C parameter at 1.

In order to estimate the generalization ability of our model, we chose a leave-one-subject-out cross-validation approach (see Supplemental File, Appendix 3). Accuracy, specificity and sensitivity were computed, as well as the area under the receiver operating characteristic curve (AUC). The AUC measures the probability that a random pair of patients and controls would be correctly identified by the classifier.

Finally, the statistical significance of the obtained classification accuracy was assessed using its null distribution under permutation testing, wherein class labels of all subjects were randomly permuted 1000 times.

2.3.3. Post-hoc analyses

- (1) Post-hoc logistic regression analyses assessing the impact of anxiety, depression and medication on classification performance: In order to ensure that our results were not driven by either medication intake, or anxiety-state and depression scores, we tested whether the STAI-S and BDI scores as well as the use of CNS-acting medication (yes or no) could predict which subject was correctly (yes or no) classified, using logistic regression. We tested the impact of these confounds individually or taken together, in all subjects and in patients only. Missing clinical scores were removed from regression analyses. We chose this procedure over the more common approach that consists of regressing out these confounds, because of the risk of removing effects that are inherent to the disorder (high rate of mood disorder co-morbidity).
- (2) Post-hoc identification of regions yielding most discriminative connections: In order to identify regions that yielded the most discriminative connections between controls and patients, we used the weights assigned by the SVM classifier to connections.
- (3) Post-hoc assessment of the connectivity differences: We sought to explore whether the sets of regions exhibiting the most discriminative connections (highest SVM weights) were hypo- or hyper-connected in patients versus controls. To do so, we calculated the average connectivity (of each group) between pairs of regions showing discriminative FC in the classification performance.
- (4) Post-hoc seed analysis exploring connectivity of right caudate: As we consistently found the right caudate as being the most discriminative region for classifying patients versus controls (Fig. 1 and Supplemental Fig. S1), we tested whether this region was differentially connected to the rest of the brain in patients versus controls. To this aim, we computed a seed-based FC analysis using the right caudate mask of the AAL atlas as the seed (see Supplemental File, Appendix 4).

3. Results

3.1. Demographic and clinical characteristics

Data from the 48 subjects (23 mFND patients and 25 controls) included in the analysis are presented in Table 1. Two patients and two controls did not complete the STAI-S and one patient and two controls did not complete the BDI. Patients did not differ from controls in terms of demographic data and anxiety scores, but showed significantly higher depression scores. Out of the 23 patients included, 14 patients took CNS-acting medication comprising either antidepressants ($n = 2$), benzodiazepine ($n = 2$), antiepileptics ($n = 4$) or a combined intake of the latter substances ($n = 5$).

3.2. Classification performance

Using whole-brain FC, we were able to distinguish mFND patients from controls with a significant accuracy (62.5 to 68.8%, Table 2).

Importantly, the individual classification performance was significant across all three atlases.

3.3. Post-hoc analyses

3.3.1. Analyses of connectivity

The most discriminative connections (i.e., those yielding the higher SVM weights) included *increased* connectivity in patients between: 1) subcortical (right caudate) and limbic (left amygdala) as well as parietal regions (bilateral postcentral gyri), 2) the paracentral lobule with frontal regions (bilateral mid orbital gyri) and *decreased* connectivity in patients between 3) parietal regions (right temporo-parietal region including the inferior parietal lobule) and frontal regions (right superior orbito-frontal gyrus), (Fig. 1).

Mean functional connectivity in controls and patients between pairs of regions showing discriminative functional connectivity (Supplemental Table S3). Discriminative connections of the other two atlases used can be found in Supplemental Fig. S1.

3.3.2. Regression analyses assessing impact of anxiety, depression and medication use

Whether subjects (either all subjects or patients only) were correctly classified or not was not predicted by depression scores or medication intake, either taken individually or altogether (Supplemental Table S2). Anxiety, however, had an impact on accuracy (when taking all subjects, but not within patients only); indeed, subjects who were more anxious were more prone to be misclassified ($\beta = -0.02$, $p = 0.0495$; see Supplemental Table S2).

3.3.3. Seed connectivity of the right caudate

In patients, the right caudate was hyper-connected to the right inferior frontal gyrus, the right and left middle orbitofrontal gyrus, the right middle cingulate cortex, the left superior parietal lobule, the left angular gyrus and the bilateral cerebellum (cf. Fig. 2/Table 3).

When contrasted to the patient group, the control group showed hyperconnectivity between the right caudate and the left hippocampus (Table 3).

4. Discussion

4.1. Classification as potential clinical diagnostic biomarker

Based on a five-minute resting-state fMRI protocol, a classification approach using the standard AAL atlas was able to discriminate mFND patients from healthy controls with almost 70% accuracy, specificity and sensitivity. Validation with two additional atlases confirmed good accuracies, i.e., 62.5–68%. Moreover, classification results were not driven by differences in depression, anxiety or psychotropic medication use.

This is the first study using a classification approach in FND. In contrast to previous fMRI studies on FND that focused on inference at the group level, the present study allows for inference at a single-subject level suited for future clinical decision-making. In recent years, classification algorithms have been applied in preclinical efforts to complement clinical diagnosis with the aim to identify neurological and psychiatric disorders using imaging-based markers (for review, (Wolfers et al., 2015)). Particularly, models based on multivariate pattern analyses of fMRI data have been proposed for several mental disorders mainly focusing on schizophrenia and mood disorders. When comparing our present findings with previous RS FC classification studies that discriminate patients from healthy controls using the same classifier (i.e., SVM), our classification accuracy and sample size range within reported values (Wolfers et al., 2015). These findings suggest that RS FC may represent a promising positive biomarker for the disorder that could be useful in future clinical practice, providing additional validation steps are followed. In particular, our findings should

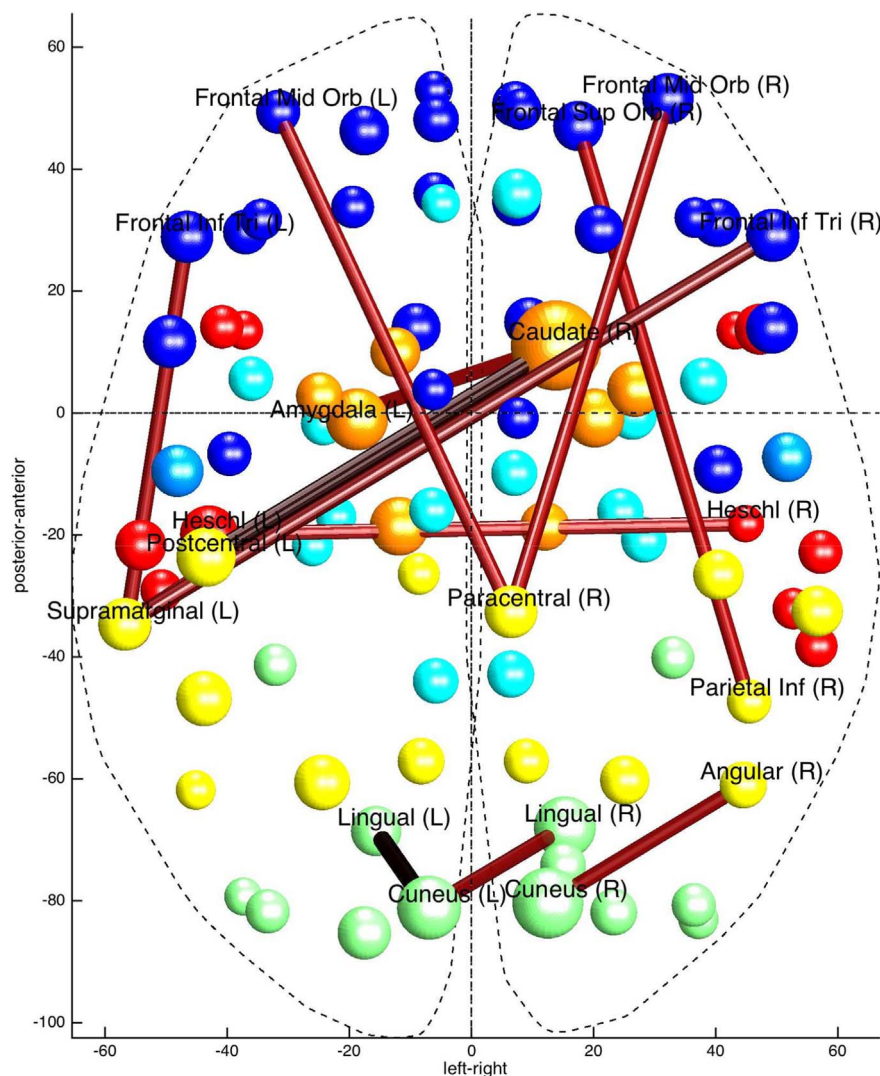


Fig. 1. Discriminative connections based on the AAL atlas. Thicker lines correspond to connections that have higher weights in classification performance. Colours of spheres correspond to different AAL lobes (blue = frontal; orange = subcortical; turquoise = limbic; yellow = parietal; red = temporal; green = occipital). (For interpretation of the references to colour in this figure legend, the reader is referred to the web version of this article.)

Table 2
Individual classification performance for all atlases.

Atlas	Accuracy (%)	Specificity (%)	Sensitivity (%)	AUC	p-value
AAL	68.8	68.0	69.6	0.72	0.004
Shirer	68.8	72.0	65.2	0.68	0.011
Hammers	62.5	68.0	56.5	0.73	0.049

AUC: area under the receiver operating characteristic (ROC) curve. The ROC curve for the individual classification obtained with each atlas can be found in Supplemental Fig. S2.

be replicated in independent and larger datasets and its reliability across different centres should be determined. It will indeed be important to verify that, when using similar acquisition parameters, the classification algorithm can be applied in another hospital. Then, a comparison not only to healthy controls but also to patients presenting the same symptom (comparing organic weakness to functional weakness for instance) should be carried out. Finally, improving specificity and sensitivity will be sought for by adding pre-test probability clinical scores and by applying feature selection (Pereira et al., 2009) and focusing on regions of interest.

4.2. Connectivity patterns to understand FND mechanisms

The primary aim of our study was to determine the value of RS FC in discriminating patients from controls at an individual level, but our

data also provide important information on a group-level to understand the underlying mechanisms of FND. Two connectivity patterns are particularly important to discuss: 1) one showing increased connectivity in patients compared to controls between the right caudate and the left amygdala and bilateral postcentral gyri and 2) one showing decreased connectivity in patients between the right inferior parietal cortex (part of the right temporo-parietal junction TPJ) and frontal regions.

4.2.1. Role of the right temporo-parietal junction (TPJ)

This latter finding of decreased connectivity between the right inferior parietal cortex and frontal regions (right superior frontal gyrus) is consistent with a recent resting state data analysis from a cohort of 25 mFND patients compared to 24 healthy controls which found decreased connectivity between the right inferior parietal cortex (taken as a seed region) and prefrontal regions (right dorsolateral prefrontal cortex/anterior cingulate) (Baek et al., 2017). Another seed-based RS FC study focused on the right TPJ in 35 mFND patients compared to 35 controls (Maurer et al., 2016) and found decreased connectivity with bilateral sensorimotor cortex, cerebellum, and right insula. The TPJ is a large region encompassing posterior inferior parietal lobule and angular gyrus (Bzdok et al., 2013). Given the role of the right TPJ in motor intention awareness and self-agency perception (Desmurget et al., 2009), aberrant connectivity involving this region might explain FND patients' inability to initiate movement and to recognize themselves as

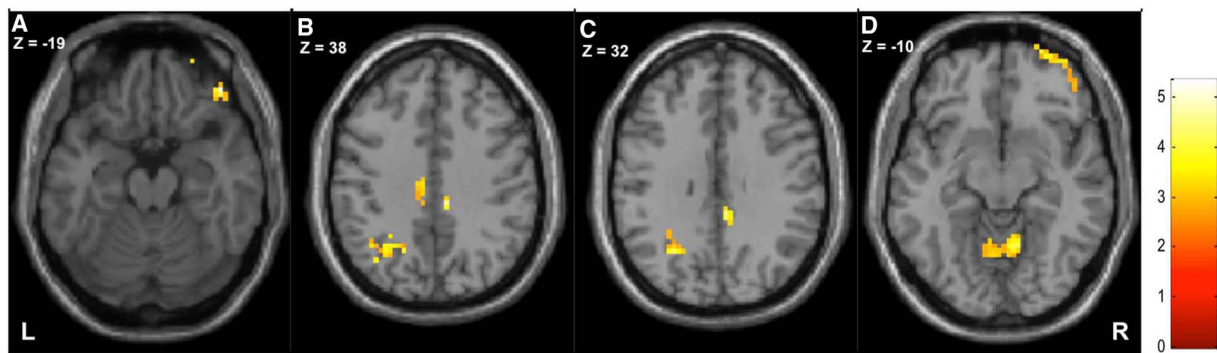


Fig. 2. Contrast patients > control in axial plane. Hyperconnectivity of clusters (listed in Supplemental Table S3) showing the right inferior frontal/orbitofrontal gyrus (A), the left parietal lobule and right mid cingulate cortex (B + C) and the bilateral cerebellum (D).

Table 3
Seed connectivity analysis of the right caudate.

p-Value	k	T	x	y	z	Region
Contrast patients > controls						
0.000	83	5.33	45	41	-19	R inferior frontal (orbitalis)
		4.59	33	62	-13	R mid orbitofrontal
		4.10	27	65	-7	R superior orbitofrontal
0.042	18	4.45	9	-31	38	R mid cingulate
		4.33	6	-37	32	R mid cingulate
0.000	61	4.26	-27	-61	32	L mid occipital
		4.25	-18	-61	41	L sup parietal lobule
		3.52	-36	-67	38	L angular gyrus
0.000	65	4.12	9	-58	-10	R cerebellum
		4.03	-3	-61	-7	L cerebellum
		2.91	-12	-58	-13	L cerebellum
		Contrast controls > patients				
0.015	26	3.87	-33	-31	-4	L hippocampus
		3.15	-36	-46	-1	L fusiform

p < 0.005 uncorrected at the peak level, p < 0.05 FDR-corrected at the cluster level, minimum cluster size = 10 voxels. K = cluster voxel size; T = t-value; x,y,z: MNI coordinates. L = left, R = right hemisphere.

the authors of their actions (Voon et al., 2010a). Our results also point to its connectivity within the executive network possibly engaged in social processing of behavior (Carter and Huettel, 2013), action awareness (Farrer et al., 2008) and top-down regulation of affects.

4.2.2. Role of the right caudate

The implication of the caudate in mFND has been previously shown in a PET experiment (Vuilleumier et al., 2001) revealing increased caudate activity during mFND with functional weakness, which returned to normal in patients who recovered from their functional weakness in a longitudinal follow-up experiment. A form of principal component analysis of these data (CY, 2011) identified a network including the thalamus and caudate (together with inferior frontal and orbitofrontal regions), which was found to exhibit selective increase in coupling in the hemisphere contralateral to the motor symptom. Another PET experiment (Schrage et al., 2013) in mFND patients with psychogenic dystonia showed abnormally increased blood flow in the basal ganglia (including the right caudate) as compared to healthy controls. The caudate, as part of the dorsal/sensorimotor striatum structure, receives many convergent excitatory projection inputs from the sensorimotor cortex, thalamus, prefrontal cortex, insula and the amygdala (Voorn et al., 2004). A proposed function of the dorsal striatum is to encode short motor programs to be linked together in order to increase complexity of motor output (Yin, 2010) thereby preventing excessive computational demands on cortical structures (Graybiel, 1998). When dysfunctional, no efficient selection and assembly of motor actions can take place, possibly resulting in abnormal

behavioral patterns, as observed in mFND. Also the caudate plays a role in favoring habitual implicit well-learned movement (McNamee et al., 2015) rather than goal-directed explicit controlled movement, a pattern observed in mFND (Parees et al., 2013). The hyperconnectivity we found between caudate and amygdala is of particular interest, as there is evidence that the amygdala plays a role in shifting goal-directed movement to habitual movement through interaction with the caudate, in order to promote well-learned defense in behavior in cases of threat (Schwabe et al., 2010). The amygdala has consistently shown increased activity in mFND (Voon et al., 2010a; Aybek et al., 2014; Voon et al., 2010b; Voon et al., 2011) as well as a lack of habituation to negative stimuli (Aybek et al., 2015). One could thus postulate that hyperarousal in mFND expressed by hyperactivity of the amygdala has an influence on motor program selection via the caudate. Our seed-based analysis on the caudate also confirms limbic-motor interaction in mFND, as it revealed hyperconnectivity with the mid-cingulate. The mid-cingulate is considered as the motor-limbic region and is thought to play a role in willed action by participating in a “choice network” (Brass et al., 2013). This region has been proposed to be a hub linking emotion (value and affects signals) to cortical and subcortical motor control (Madlon-Kay et al., 2013).

Altogether, RS FC data from our study and previous literature confirm findings from task-based fMRI experiments involving nodes of motor control (self-agency, motor intention and motor action selection) with limbic system key regions (amygdala, motor mid-cingulate cortex).

4.3. Limitations

Our study has several limitations. One is the homogenous sample of adult subjects suffering from mFND, not including other FND presentation such as non-epileptic seizure and not including children, which limits the generalizability of our findings to FND in general. Also, the fact that our patients had similar anxiety scores to controls suggests that our cohort may not be representative of FND in general, who tend to be more anxious. A future design should aim to include all consecutive patients and monitor drop-outs (rate and reason) in order to ensure the studied population is representative of the general FND population.

Another limitation is the fact that our sample included both positive (movements) and negative (weakness), which may confound the results. This may be overcome in future validation steps by including larger number of patients and stratifying them according to symptom type.

Another limitation is that we included patients with psychotropic medication. Although we verified with post-hoc analyses that classification results were not driven by medication, we cannot be certain that drug intake did not affect our results. Similarly, we verified that depression scores did not predict the classification - future studies should

exclude that this variable is not a confounding factor. Another limitation of our study is the rather small sample size (total of 48 subjects) that could directly affect classifier performance and lead to unstable predictive models. However, in a large comprehensive review of studies using classifiers in neuropsychiatry, sample sizes were mostly below 100 with a majority of sample sizes around 50 participants (Wolfers et al., 2015).

4.4. Conclusions

Classification using resting state fMRI allowed for discrimination of mFND patients from healthy controls with almost 70% accuracy, specificity and sensitivity.

This constitutes an important first step towards clinical application of such a non-invasive technique, not to replace the clinical diagnosis but to ascertain its value and to provide additional rule-in tests to make the diagnosis of mFND. Future validation steps are now needed in separate samples and other MRI scanners, as well as in combination with clinical scores (pre-test probability) to confirm that this classification tool can be utilized in clinics worldwide.

Conflicts of interest

None.

Funding/support

This work was supported by the Swiss National Research Foundation (Ambizione grant PZ00P3_147997 for SA) and the Leenards Nested Project grant.

Supplementary data

Supplementary data to this article can be found online at <https://doi.org/10.1016/j.nicl.2017.10.012>.

References

- Aleman-Gomez, Y.M.-G., Melie-Garcia, L., Valdés-Hernandez, P., 2006. IBASPM: toolbox for automatic parcellation of brain structures. In: Annual Meeting of the Organization for Human Brain Mapping. 27 Florence, Italy.
- Aybek, S., Nicholson, T.R., Zelaya, F., O'Daly, O.G., Craig, T.J., David, A.S., et al., 2014. Neural correlates of recall of life events in conversion disorder. *JAMA Psychiat.* 71 (1), 52–60.
- Aybek, S., Nicholson, T.R., O'Daly, O., Zelaya, F., Kanaan, R.A., David, A.S., 2015. Emotion-motion interactions in conversion disorder: an fMRI study. *PLoS One* 10 (4), e0123273.
- Baek, K., Donamayor, N., Morris, L.S., Strelchuk, D., Mitchell, S., Mikheenko, Y., et al., 2017. Impaired awareness of motor intention in functional neurological disorder: implications for voluntary and functional movement. *Psychol. Med.* 1–13.
- Beck, A.T.S., Steera, R.A., Brown, G., 1996. Manual for the Back Depression Inventory-II. Psychological Corporation, San Antonio, TX.
- Brass, M., Lynn, M.T., Demanet, J., Rigoni, D., 2013. Imaging volition: what the brain can tell us about the will. *Exp. Brain Res.* 229 (3), 301–312.
- Bzdok, D., Langner, R., Schilbach, L., Jakobs, O., Roski, C., Caspers, S., et al., 2013. Characterization of the temporo-parietal junction by combining data-driven parcellation, complementary connectivity analyses, and functional decoding. *NeuroImage* 81, 381–392.
- Carson, A., Stone, J., Hibberd, C., Murray, G., Duncan, R., Coleman, R., et al., 2011. Disability, distress and unemployment in neurology outpatients with symptoms 'unexplained by organic disease'. *J. Neurol. Neurosurg. Psychiatry* 82 (7), 810–813.
- Carter, R.M., Huettel, S.A., 2013. Nexus model of the temporal-parietal junction. *Trends Cogn. Sci.* 17 (7), 328–336.
- CDG, Spielberger, Gorsuch, R.L., Lushene, R., Vagg, P.R., Jacobs, G.A., 1983. Manual for the State-Trait Anxiety Inventory. Consulting Psychologists Press, Palo Alto, CA.
- Crimlisk, H.L., Bhatia, K.P., Cope, H., David, A.S., Marsden, D., Ron, M.A., 2000. Patterns of referral in patients with medically unexplained motor symptoms. *J. Psychosom. Res.* 49 (3), 217–219.
- CY, Vuilleumier P., 2011. In: Hallett CC, M., Fahn, S. (Eds.), *Functional Brain-imaging of Psychogenic Paralysis During Conversion and Hypnosis*. Cambridge University Press.
- Daum, C., Hubschmid, M., Aybek, S., 2014. The value of 'positive' clinical signs for weakness, sensory and gait disorders in conversion disorder: a systematic and narrative review. *J. Neurol. Neurosurg. Psychiatry* 85 (2), 180–190.
- Desmurget, M., Reilly, K.T., Richard, N., Szathmari, A., Mottolese, C., Sirigu, A., 2009. Movement intention after parietal cortex stimulation in humans. *Science* 324 (5928), 811–813.
- Espay, A.J., Goldenhar, L.M., Voon, V., Schrag, A., Burton, N., Lang, A.E., 2009. Opinions and clinical practices related to diagnosing and managing patients with psychogenic movement disorders: an international survey of movement disorder society members. *Mov. Disord.* 24 (9), 1366–1374.
- Farrer, C., Frey, S.H., Van Horn, J.D., Tunik, E., Turk, D., Inati, S., et al., 2008. The angular gyrus computes action awareness representations. *Cereb. Cortex* 18 (2), 254–261.
- Gelauff, J., Stone, J., Edwards, M., Carson, A., 2014. The prognosis of functional (psychogenic) motor symptoms: a systematic review. *J. Neurol. Neurosurg. Psychiatry* 85 (2), 220–226.
- Graybiel, A.M., 1998. The basal ganglia and chunking of action repertoires. *Neurobiol. Learn. Mem.* 70 (1–2), 119–136.
- Hammers, A., Allom, R., Koepp, M.J., Free, S.L., Myers, R., Lemieux, L., et al., 2003. Three-dimensional maximum probability atlas of the human brain, with particular reference to the temporal lobe. *Hum. Brain Mapp.* 19 (4), 224–247.
- Kanaan, R., Armstrong, D., Wessely, S., 2009a. Limits to truth-telling: neurologists' communication in conversion disorder. *Patient Educ. Couns.* 77 (2), 296–301.
- Kanaan, R., Armstrong, D., Barnes, P., Wessely, S., 2009b. In the psychiatrist's chair: how neurologists understand conversion disorder. *Brain J. Neurol.* 132 (Pt 10), 2889–2896.
- Madlon-Kay, S., Pesaran, B., Daw, N.D., 2013. Action selection in multi-effector decision making. *NeuroImage* 70, 66–79.
- Maurer, C.W., LaFaver, K., Ameli, R., Epstein, S.A., Hallett, M., Horowitz, S.G., 2016. Impaired self-agency in functional movement disorders: a resting-state fMRI study. *Neurology* 87 (6), 564–570.
- McNamee, D., Liljeholm, M., Zika, O., O'Doherty, J.P., 2015. Characterizing the associative content of brain structures involved in habitual and goal-directed actions in humans: a multivariate fMRI study. *J. Neurosci.* 35 (9), 3764–3771.
- Parees, I., Kassavetis, P., Saifee, T.A., Sadnicka, A., Davare, M., Bhatia, K.P., et al., 2013. Failure of explicit movement control in patients with functional motor symptoms. *Mov. Disord.* 28 (4), 517–523.
- Pereira, F., Mitchell, T., Botvinick, M., 2009. Machine learning classifiers and fMRI: a tutorial overview. *NeuroImage* 45 (1 Suppl), S199–209.
- Richiardi, J., Gschwind, M., Simioni, S., Annoni, J.M., Greco, B., Hagmann, P., et al., 2012. Classifying minimally disabled multiple sclerosis patients from resting state functional connectivity. *NeuroImage* 62 (3), 2021–2033.
- Schrag, A.E., Mehta, A.R., Bhatia, K.P., Brown, R.J., Frackowiak, R.S., Trimble, M.R., et al., 2013. The functional neuroimaging correlates of psychogenic versus organic dystonia. *Brain J. Neurol.* 136 (Pt 3), 770–781.
- Schwabe, L., Tegenthoff, M., Hoffken, O., Wolf, O.T., 2010. Concurrent glucocorticoid and noradrenergic activity shifts instrumental behavior from goal-directed to habitual control. *J. Neurosci.* 30 (24), 8190–8196.
- Shirer, W.R., Ryali, S., Rykhlevskaia, E., Menon, V., Greicius, M.D., 2012. Decoding subject-driven cognitive states with whole-brain connectivity patterns. *Cereb. Cortex* 22 (1), 158–165.
- Slater, E., 1965. Diagnosis of "hysteria". *Br. Med. J.* 1 (5447), 1395–1399.
- Stone, J., Carson, A., Duncan, R., Coleman, R., Roberts, R., Warlow, C., et al., 2009. Symptoms 'unexplained by organic disease' in 1144 new neurology out-patients: how often does the diagnosis change at follow-up? *Brain J. Neurol.* 132 (Pt 10), 2878–2888.
- Tzourio-Mazoyer, N., Landeau, B., Papathanassiou, D., Crivello, F., Etard, O., Delcroix, N., et al., 2002. Automated anatomical labeling of activations in SPM using a macroscopic anatomical parcellation of the MNI MRI single-subject brain. *NeuroImage* 15 (1), 273–289.
- Voon, V., Gallea, C., Hattori, N., Bruno, M., Ekanayake, V., Hallett, M., 2010a. The involuntary nature of conversion disorder. *Neurology* 74 (3), 223–228.
- Voon, V., Brezing, C., Gallea, C., Ameli, R., Roelofs, K., WC Jr., LaFrance, et al., 2010b. Emotional stimuli and motor conversion disorder. *Brain J. Neurol.* 133 (Pt 5), 1526–1536.
- Voon, V., Brezing, C., Gallea, C., Hallett, M., 2011. Aberrant supplementary motor complex and limbic activity during motor preparation in motor conversion disorder. *Mov. Disord.* 26 (13), 2396–2403.
- Voorn, P., Vanderschuren, L.J., Groenewegen, H.J., Robbins, T.W., Pennartz, C.M., 2004. Putting a spin on the dorsal-ventral divide of the striatum. *Trends Neurosci.* 27 (8), 468–474.
- Vroomen, P.C., Buddingh, M.K., Luijckx, G.J., De Keyser, J., 2008. The incidence of stroke mimics among stroke department admissions in relation to age group. *J. Stroke Cerebrovasc. Dis.* 17 (6), 418–422.
- Vuilleumier, P., Chicherio, C., Assal, F., Schwartz, S., Slosman, D., Landis, T., 2001. Functional neuroanatomical correlates of hysterical sensorimotor loss. *Brain J. Neurol.* 124 (Pt 6), 1077–1090.
- Wolfers, T., Buitelaar, J.K., Beckmann, C.F., Franke, B., Marquand, A.F., 2015. From estimating activation locality to predicting disorder: a review of pattern recognition for neuroimaging-based psychiatric diagnostics. *Neurosci. Biobehav. Rev.* 57, 328–349.
- Woodward, N.D., Cascio, C.J., 2015. Resting-state functional connectivity in psychiatric disorders. *JAMA Psychiat.* 72 (8), 743–744.
- Yin, H.H., 2010. The sensorimotor striatum is necessary for serial order learning. *J. Neurosci.* 30 (44), 14719–14723.